

C. NEUS¹, W. FOUBERT¹, Y. ROLAIN¹, J. MAES², L. VAN BIESEN¹

¹Department of Fundamental Electricity and Instrumentation, Vrije Universiteit Brussel
Brussel, Belgium

²Bell Labs Antwerp, Alcatel-Lucent
Antwerp, Belgium

e-mail: cneus@vub.ac.be, wfoubert@vub.ac.be, yrolain@vub.ac.be, jochen.maes@alcatel-lucent.be,
lvbiesen@vub.ac.be

FEASIBILITY AND CHALLENGES OF DSL LOOP MAKE-UP IDENTIFICATION VIA SINGLE-ENDED LINE TESTS

Digital subscriber lines (DSL) offer the possibility to deliver broadband services over the existing telephone network. Yet, before deploying DSL, the subscriber loops must be tested to see if they can support high-speed data services, and at what rate. Single-ended automatic qualification is essential to achieve low-cost deployment of DSL, since it allows loops to be qualified in bulk without human intervention at the customer's location. An even more ambitious challenge is to fully characterize the loop, i.e. to identify its composition completely (number of loop sections, length and cable type of each section). This paper discusses the feasibility and the challenges of loop make-up identification via single-ended measurements.

Keywords: Digital Subscriber Lines (DSL), Single-Ended Line Testing (SELT), reflectometry, near-end reflection, dispersion.

1. INTRODUCTION

Nowadays, Digital Subscriber Line (DSL) technology is one of the ways to offer broadband services, e.g. internet or video-on-demand. DSL exploits the telephone network of the subscriber to transport the high-speed data. Yet, before deploying DSL to a new customer, the subscriber loop must be tested to see if it can support the considered DSL service. This process is called 'loop qualification' and the outcome will be different for each customer since it depends on the subscriber loop, i.e. the twisted pair cables connecting the customer premises to the central office. Many loop make-ups are possible, but in Europe a subscriber loop most often consists of a cascade of several line sections with increasing diameter (gauge) from the central office towards the customer [1]. Identifying the make-up of a subscriber loop (number of sections, length and gauge of each section) is not only important for a realistic capacity estimation, but can also

¹ Received: October 14, 2008. Revised: November 26, 2008.

benefit network planning, maintenance and diagnosis of loop impairments in general. Single-ended line testing (SELT) is often preferred over dual-ended line testing (DELT) for loop qualification, as it eliminates the necessity of dispatching a technician to the customer's site [2]. The tests can then also be run periodically from the central office, to test the loops in bulk without any human intervention.

The theoretical channel capacity of a subscriber loop is given by Shannon's formula [3]:

$$C = \int_{f_1}^{f_2} \log_2 \left(1 + \frac{|H(f)|^2 S(f)}{N(f)} \right) df, \quad (1)$$

with $S(f)$ the transmit power, $N(f)$ the noise power and $H(f)$ the transfer function of the channel. In other words, $\frac{|H(f)|^2 S(f)}{N(f)}$ is the received signal-to-noise ratio. $[f_1, f_2]$ is the frequency band in which the DSL service operates, e.g. [25.875 kHz, 2.208 MHz] for ADSL2+. The disadvantage of SELT is that, in contrast to DELT, the transfer function $H(f)$ cannot be measured directly, but should be estimated instead. The transfer function depends on the make-up of the subscriber loop and as such, with SELT the key issue is to identify the composition of the subscriber loop (number of cable sections, length and gauge of each section) from the measurements. Once the loop make-up has been estimated, the transfer function $H(f)$ can easily be calculated using the ABCD parameters of the channel [4].

The underlying physical phenomenon that allows estimation of the loop make-up with SELT is that gauge changes and the end of the loop represent a discontinuity in the transmission line that will result in an abrupt change of the characteristic impedance of the loop. As a result, when a signal is injected into the subscriber loop, every discontinuity will generate a reflection, as can be seen in Fig. 1. The analysis of these echoes allows (at least in theory) inducing the complete loop make-up for a cascade of lines.

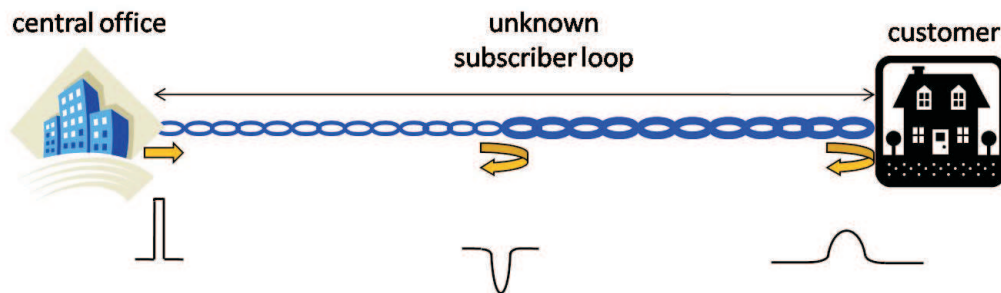


Fig. 1. Basic principle of reflectometry applied to a subscriber loop consisting of a cascade of two line segments.

Reflectometry is a general concept. By consequence, it can be implemented in several different ways. There are few papers in literature addressing the problem of subscriber loop make-up estimation through single-ended tests. Galli et al [5], [6] use time domain reflectometry (TDR) with a square pulse as the excitation signal. Consequently, the measured reflections are dependent on the shape of the injected pulse. Boets et al propose to use the one-port scattering parameter $S_{11}(f)$ to get rid of the dependence on the shape of the input pulse. As $S_{11}(f)$ is a relative quantity (the ratio of the reflected to the injected voltage wave), its determination performs a deconvolution of the measured output spectrum and provides a better indicator of the loop make-up [2], [7]. Here, the excitation signals are discrete multitones (DMT) placed on the ADSL frequency grid. Another measurement technique, proposed by Dodds et al [8], energizes the loop with a sinusoid whose frequency increases in a number of discrete steps and measures the reflections through coherent detection. Both latter measurement techniques can be catalogued as frequency domain reflectometry (FDR) techniques. Nevertheless, independently of the chosen implementation method, one encounters difficulties when attempting to identify the loop make-up. In this paper we discuss the main problems, in both the time and the frequency domain. As will be shown in this paper, the evaluation of the loop make-up is challenging, even for very simple cases.

The remainder of this paper is structured as follows. Section 2 gives some theoretical background and states the main challenges: the near-end reflection, the dispersion and the spatial resolution. These are detailed further in Sections 3, 4 and 5 respectively. Section 6 summarizes the most important conclusions.

2. PROBLEM STATEMENT

With single-ended line testing all measurements are performed from the central office and as a consequence the subscriber loop should be considered to act as a one-port. All the information that can be acquired about the loop through this port is contained in the one-port scattering parameter $S_{11}(f)$, which is the ratio of the reflected voltage wave to the incident voltage wave. The one-port scattering parameter can be measured by means of a network analyzer in the frequency domain. If the subscriber loop consists of a single line, then this transmission line can be modelled as follows [2]:

$$S_{11}(f) = \frac{-\rho_g + \rho_L e^{-2\gamma l}}{1 - \rho_g \rho_L e^{-2\gamma l}}. \quad (2)$$

Herein, l is the unknown length of the line and γ is the propagation constant of the line. The reflection factor ρ_g at the measurement device plane and the reflection factor ρ_L at the line end are given by:

$$\rho_g = \frac{Z_g - Z_c}{Z_g + Z_c} \quad \text{and} \quad \rho_L = \frac{Z_L - Z_c}{Z_L + Z_c}, \quad (3)$$

with Z_g the impedance of the measurement device, Z_c the characteristic impedance of the transmission line and Z_L the load impedance that is present at the line end, as shown in Fig. 2.

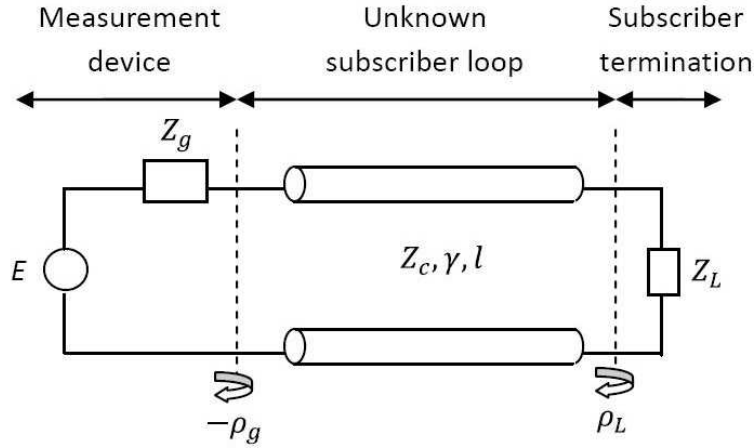


Fig. 2. Reflections for a subscriber loop consisting of a single line.

We can now perform the series expansion $\frac{1}{1+x} = 1 - x + x^2 - \dots$ on (2) if we make the assumption that the reflections are small ($\rho_g \rho_L e^{-2\gamma l} < 1$):

$$\begin{aligned} S_{11}(f) &= (-\rho_g + \rho_L e^{-2\gamma l}) (1 + \rho_g \rho_L e^{-2\gamma l} + \dots) \\ &= -\rho_g + \rho_L (1 - \rho_g^2) e^{-2\gamma l} + \text{multiple reflections} \end{aligned} \quad (4)$$

We then obtain a structure which allows easy interpretation. Note that the formulas are expressed in the frequency domain, but performing the inverse Fourier transform (IFFT) gives the reflectogram. As such, the reader can interpret (4) in the time domain as well. The first term in (4) represents the reflection at the measurement device, due to the impedance mismatch between the measurement device and the line. The second term is the reflection created by the line end, which is the actual meaningful reflection containing information about the line length l . We will also receive multiples of this reflection because the signal bounces back and forth on the line.

We can then rewrite (4) with the complex propagation constant $\gamma = \alpha + j\beta$. The following assumptions are made to keep the example simple without loss of generality:

- we ignore the multiple reflections (because the attenuation strongly increases with every multiple reflection and as such only a few multiples (if any) will be visible);
- we neglect ρ_g^2 (because it is much smaller than in most cases);

- c) we assume the line end to be open (as is the case for an on-hooked telephone), resulting in $\rho_L = 1$.

Therefore, $S_{11}(f)$ for a single line simplifies to:

$$S_{11}(f) \approx -\rho_g + e^{-2\alpha l} e^{-2j\beta l}. \quad (5)$$

Since in general ρ_g is a complex function of the frequency, we can write the real and imaginary parts of $S_{11}(f)$ as:

$$\Re \{S_{11}(f)\} = -\Re \{\rho_g\} + e^{-2\alpha l} \cos(-2\beta l). \quad (6)$$

$$\Im \{S_{11}(f)\} = -\Im \{\rho_g\} + e^{-2\alpha l} \sin(-2\beta l). \quad (7)$$

Although (6) and (7) do not look very complicated, it is still hard to identify the line length l precisely from them. The first problem we encounter is the unwanted reflection that is present at the measurement device. Section 3 will describe the influence of this term in more detail. Secondly, the unknown parameter l is present in the exponent as well as in the sinusoidal function. Since the attenuation constant $\alpha(f)$ and the phase constant $\beta(f)$ are frequency dependent, a classical signal parameter estimation is impossible. Moreover, if the gauge type is not known a priori, then $\alpha(f)$ and $\beta(f)$ are also unknown and have to be estimated as well. Section 4 will focus on the estimation of the line length l . To conclude, section 5 will discuss the importance of the measurement bandwidth in the loop make-up estimation.

3. NEAR-END REFLECTION

In general, the measurement device is not matched to the loop under test. The measured one-port scattering parameter of the subscriber loop is expressed in reference impedance Z_g , which is typically 50Ω , while the characteristic impedance Z_c of a twisted pair copper telephone cable varies around 115Ω . This impedance mismatch will generate a reflection at the interface of the measurement device, called the “near-end reflection” (first term in (6) and (7)). This near-end reflection might mask the reflection of the line end in the frequency domain as well as the time domain, especially for long lines [5],[7]. The top rows of Fig. 3 illustrate this problem for a single line of 1800 m with a diameter of 0.4 mm.

If a calibration is performed, then $S_{11}(f)$ is expressed using the calibration load as the reference impedance, which can be chosen to match more closely the impedance of the line. However, the measurement device can never perfectly be matched to the loop under test as the line type is unknown a priori and moreover, the characteristic impedance of the line is a highly frequency dependent function [9].

Several approaches are possible to tackle this problem. In [7], the impedance in which the measured scattering parameter $S_{11,meas}$ is expressed is changed to match the

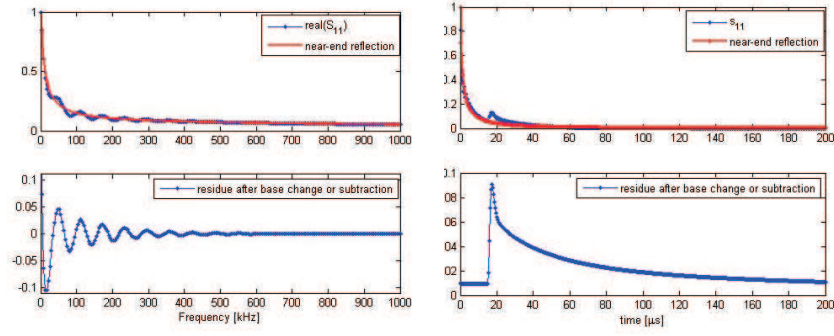


Fig. 3. Near-end reflection partially masking the line end reflection of a 1800 m line (top) in the frequency domain (left) and in the time domain (right); after base change or subtraction of the near-end reflection, the end reflection becomes more clearly visible (bottom).

characteristic impedance of the line as closely as possible ($Z_{new} \approx Z_c$). This is done through post-processing using (8). For this, the characteristic impedance $Z_c(f)$ of the line needs to be estimated first, and $S_{11}(f)$ is then expressed using this impedance Z_{new} as a reference impedance.

$$S_{11}|_{Z_{new}} = \frac{Z_g \left(\frac{1+S_{11,meas}}{1-S_{11,meas}} \right) - Z_{new}}{Z_g \left(\frac{1+S_{11,meas}}{1-S_{11,meas}} \right) + Z_{new}}. \quad (8)$$

In [5] and [8] the near-end reflection ρ_g is estimated by measuring a very long line, in the time and frequency domain respectively. The near-end reflection is then subtracted from the original one-port scattering parameter measurement. This assumes that a very long line of similar type is available and this is not always true in practice. Another possibility is to fit the near-end reflection first to subtract it afterwards. In [10] a rational function of order 2/1 was used and gave satisfactory results for a wide range of loop make-ups. The bottom figures of Fig. 3 show the residue signal after removal of the near-end reflection.

In any case, it is important to remove the near-end reflection ρ_g or at least reduce it as much as possible to ease the identification of the loop make-up.

4. DISPERSION

When considering a subscriber loop made up of a cascade of line segments with different gauges, it is important to keep the reflections as narrow as possible to ease the identification procedure. This is necessary to be able to resolve two closely separated reflections and to be able to distinguish a small reflection in the proximity of a large one. Fig. 4 shows the reflectogram for a cascade of a 2000 m cable with a diameter of 0.4 mm, a 1000 m cable with a diameter of 0.5 mm and a 1000 m cable with a

diameter of 0.6 mm. If nothing is done to compensate for the dispersion, the second reflection is difficult (if not impossible) to detect. The three reflections, with reduced dispersion, are added for illustrative purposes.

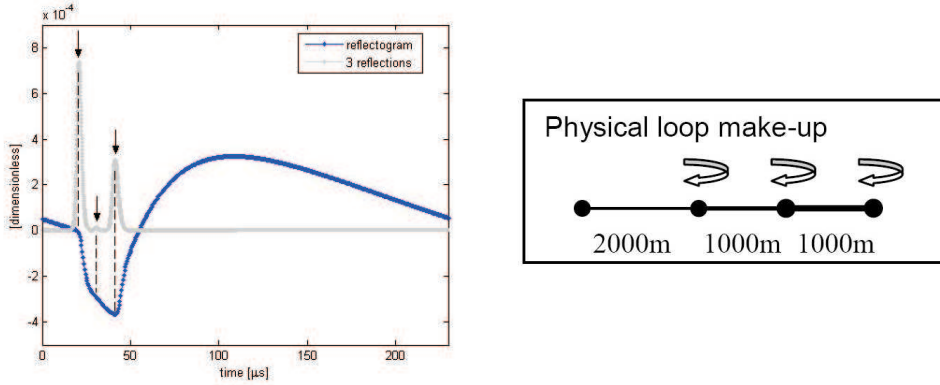


Fig. 4. Reflectogram for a simulated cascade of 2000 m (0.4 mm), 1000 m (0.5 mm) and 1000 m (0.6 mm). The three reflections, with reduced dispersion, are added for illustrative purposes.

To determine the factors that influence the dispersion and hence define the width of a reflection, we return to the example of the single line. Once the near-end reflection is removed, formulas (6) and (7) further simplify to:

$$\Re \{S_{11}(f)\} = e^{-2\alpha(f)l} \cos(-2\beta(f)l). \quad (9)$$

$$\Im \{S_{11}(f)\} = e^{-2\alpha(f)l} \sin(-2\beta(f)l). \quad (10)$$

This means that for a single line, the one-port scattering parameter is a damped sinusoid. The exponential term reflects the attenuation of the line and depends on the attenuation constant $\alpha(f)$ and the line length l . The sinusoidal term represents the standing waves created on the line due to the excitation. It depends on the line length l , as well as on the phase constant $\beta(f)$. Note that $\alpha(f)$ and $\beta(f)$ are frequency dependent, and are not constants as their name would suggest.

4.1. Phase constant $\beta(f)$

If the phase constant $\beta(f)$ were perfectly linear ($\beta = m \cdot f$ with $m \in \mathbf{R}$), we would have a perfect sine with one “time” component. In the time domain, this means we would have a Dirac pulse at time instant $t^\bullet = ml/\pi$. This can then be exactly related to the unknown line length l through the propagation speed v_p of the line:

$$l = \frac{v_p t^\bullet}{2}. \quad (11)$$

Unfortunately, in practice $\beta(f)$ is not a linear function of the frequency. As a consequence, we have a sinusoid with some time modulation. This means that in the time domain, the reflection will not be a Dirac pulse, but rather will have a certain finite width. This phenomenon is well known as pulse dispersion [11], and is often explained by stating that it results from the fact that the propagation speed $v_p(f)$ is not a constant. As can be seen in (12), if $\beta \neq m \cdot f$, the propagation speed v_p is indeed frequency-dependent.

$$v_p(f) = \frac{2\pi f}{\beta(f)}. \quad (12)$$

Measuring the one-port scattering parameter in the frequency domain and performing an IFFT corresponds to measuring the reflectogram in the time domain by exciting it with a sharp impulse. The traveling impulse will be strongly influenced by the dispersion, thus causing broad reflections. However, this broadening can be diminished if we apply a whitener function to $S_{11}(f)$ in the frequency domain. This corresponds with the use of an equalizer in the time domain, as is commonly used in DSL modems to counteract the channel dispersion and avoid intersymbol interference [4], [12].

4.2. Attenuation constant $\alpha(f)$

The exponential attenuation factor in (9) and (10) will increase the distortion of the ideal sinusoid even more. The fact that the attenuation constant $\alpha(f)$ is not constant, as its name would suggest, but strongly frequency-dependent, causes supplementary dispersion in the time domain. In theory, the attenuation could be compensated by multiplying the signal with a factor $e^{2\alpha(f)l}$. However, this can only be done when the unknown line length has already been estimated and the attenuation constant $\alpha(f)$ is known. The compensation of the losses then results in an improvement in spatial resolution, from which the identification can benefit. An alternative approach would be to estimate the envelope of $S_{11}(f)$ and to compensate by multiplying by its inverse function. This way, the attenuation is also countered.

Fig. 5 shows the frequency dependence of the attenuation constant $\alpha(f)$ and the propagation speed $v_p(f)$. Fig. 6 gives a graphical overview of the two factors causing dispersion in the time domain. These two influences can be separated in the frequency domain, as discussed above. In contrast, in the time domain they are inseparable.

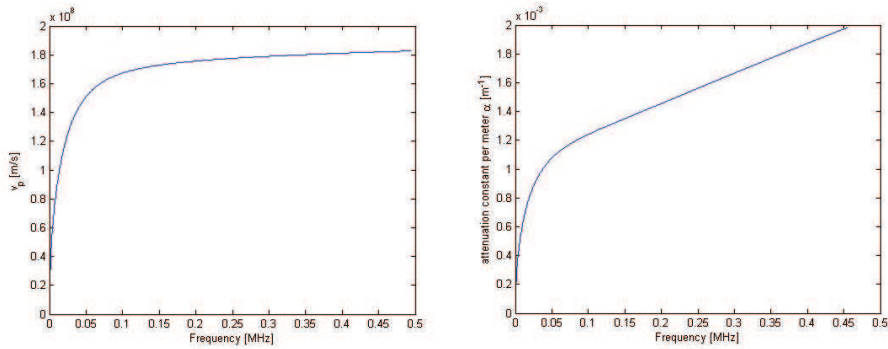


Fig. 5. The frequency dependent propagation speed (left) and attenuation constant (right) cause dispersion on the subscriber loop.

	Frequency domain	Time domain
$\sin(-2\beta(f)l)$ with $\beta = m \cdot f$	<p>A plot of a pure sinusoid with constant amplitude and frequency over a range of 0 to 500 kHz.</p>	<p>A plot of a sharp, narrow impulse in the time domain.</p>
$\sin(-2\beta(f)l)$ with $\beta \neq m \cdot f$	<p>A plot of a sinusoid whose frequency varies with frequency, causing the period to change across the spectrum.</p>	<p>A plot of a pulse in the time domain that is significantly dispersed and broadened.</p>
$e^{-2\alpha(f)l} \sin(-2\beta(f)l)$ with $\beta \neq m \cdot f$ and $\alpha(f) \neq \text{constant}$	<p>A plot of a sinusoid whose amplitude decays as frequency increases, representing frequency-dependent damping.</p>	<p>A plot of a smooth, broadened pulse in the time domain, showing significant dispersion.</p>

Fig. 6. We are dealing with a sinusoid with time modulation and frequency dependent damping. This causes dispersion in the time domain.

5. SPATIAL RESOLUTION

Fig. 7 shows a typical setup as it is present at the central office. The voice signals of the Plain Old Telephony Service (POTS) are separated from the DSL data by a splitter. If the measurement device can be placed between the splitter and the Main Distribution Frame, then the response of the line over the complete measured frequency band can be used. However, this is often not possible (e.g. for competitive local exchange carriers) and the measurement device will more probably be placed in the Digital Subscriber Line Access Multiplexer (DSLAM). As a consequence, for test purposes, the low frequencies will be missing or will be distorted [1], [13].

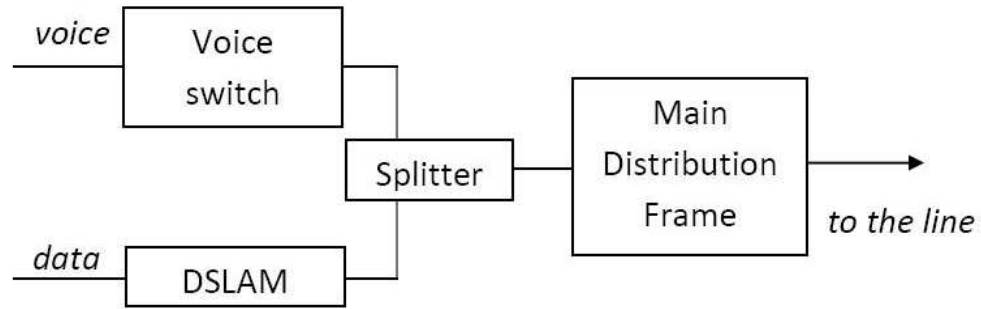


Fig. 7. Splitting of voice and data at the central office.

Besides the problem of the missing low frequency information, the maximal frequency is also bounded by practical implementation issues. Firstly, the maximal frequency is described in the standards of the considered DSL technology and sending energy outside this band is not allowed [14], [15]. Secondly, the signal-to-noise ratio (SNR) also constrains the maximal usable frequency, as the line attenuation strongly increases with frequency (see Fig. 5).

Anyhow, only a part of the measured frequency band will be reliable and should be used for the identification. This will again adversely affect the spatial resolution, as it is inversely proportional to the used frequency band.

$$L_{resolution} = \left(\frac{1}{f_{max} - f_{min}} \right) \frac{v_p}{2} \quad (13)$$

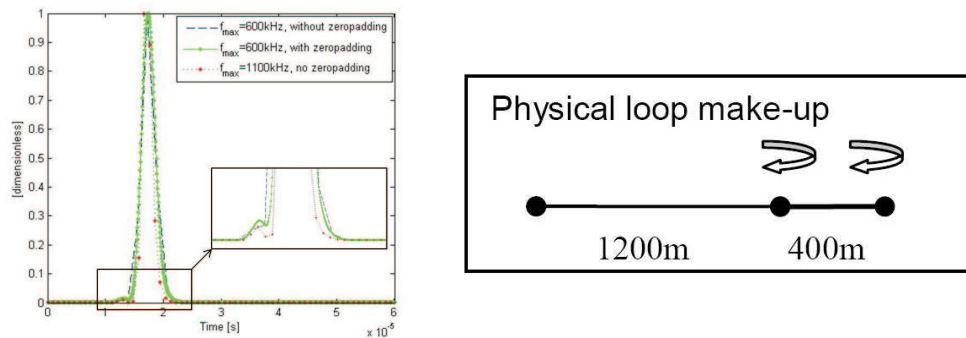


Fig. 8. A 1200 m 0.4 mm line cascaded with a 400 m 0.5 mm line. The time resolution can be improved by increasing f_{max} (often not possible in practice) or zero padding.

A good resolution in the time domain is highly desirable to attain a high resolvability, especially when the reflections are in each other's proximity, as already discussed

in Section 4. The problem is that in practical situations, the usable frequency band might be quite small. If, for example the voice band signals are suppressed by the splitter ($f_{\min} = 25$ kHz) and the maximal frequency is limited to $f_{\max} = 600$ kHz due to SNR considerations, this would only allow for a spatial resolution of 175 m, which is often insufficient. If the maximal frequency cannot be increased any further, then zero padding can be a solution to artificially extend the data sequence. Fig. 8 shows a simulation example: a 1200 m 0.4 mm line cascaded with a 400 m 0.5 mm line. When the data record is not extended by increasing f_{\max} or by zero padding, then the two reflections cannot be resolved. It should be noted that zero padding does not introduce any new information, but it only improves the visibility of the reflections.

6. CONCLUSIONS

In this paper we have addressed the major challenges that are encountered when attempting to identify the make-up of a subscriber loop with single-ended measurements. Even in the most simple case, namely a single line, the near-end reflection might mask the reflection from the loop end. Moreover, when performing an inverse Fourier transform on the measured one-port scattering parameter $S_{11}(f)$, we do not obtain a Dirac pulse corresponding to the reflection, but rather a lobe around this location. There are two main reasons for this dispersion.

1. The phase characteristic of the line is not linear as a function of the frequency.
2. The line attenuation is frequency dependent.

The measurement bandwidth should also be considered, to ensure sufficient spatial resolution.

These drawbacks are not a major problem for a single line. On the contrary, if we consider cascades of lines, as is mostly the case in subscriber loops, more than one reflection is present. It is then of uttermost importance to keep the reflections as small as possible to attain a high resolvability, especially when the reflections are in each other's proximity. Once the loop make-up has been estimated, the loop capacity can be calculated with Shannon's formula. A good estimation of the subscriber loop capacity is important for telephone companies providing DSL services, in order to have a tool to assess the capability of a subscriber loop in carrying DSL services.

ACKNOWLEDGMENT

This research was carried out in the framework of the IWT project "iSEED: Innovation on Stability, Spectral and Energy Efficiency in DSL".

REFERENCES

1. Starr T., Sorbara M., Cioffi J., Silverman P.: *DSL Advances*. Upper Saddle River, 2003, pp. 262–265.
2. Bostoën T., Boets P., Zekri M., Van Biesen L., Pollet T., Rabijns D.: “Estimation of the Transfer Function of a Subscriber Loop by Means of One-Port Scattering Parameter Measurement at the Central Office”, *IEEE Journal on Selected Areas in Communications*, vol. 20, no. 5, 2002, pp. 936–948.
3. Golden P., Dedieu H., Jacobsen K.: *Implementation and Applications of DSL Technology*. Auerbach Publications, 2008, pp. 576–577.
4. Chen W.Y.: *DSL: Simulation Techniques and Standards Development for Digital Subscriber Line Systems*. MacMillan Technical Publishing, 1998, pp. 41–53.
5. Galli S., Waring D.L.: “Loop Makeup Identification Via Single Ended Testing: Beyond Mere Loop Qualification”, *IEEE Journal on Selected Areas in Communications*, vol. 20, no. 5, 2002, pp. 923–935.
6. Galli S., Kerpez K.J.: “Single-Ended Loop Make-Up Identification”, *IEEE Transactions on Instrumentation and Measurement*, vol. 55, no. 2, 2006, pp. 528–549.
7. Boets P., Bostoën T., Van Biesen L., Pollet T.: “Pre-Processing of Signals for Single-Ended Subscriber Line Testing”, *IEEE Transactions on Instrumentations and Measurement*, vol. 55, no. 5, 2006, pp. 1509–1518.
8. Celaya B., Dodds D.: “Single-Ended DSL Line Tester”, Proceedings of Canadian Conference on Electrical and Computer Engineering, Niagara Falls, 2004, pp. 2155–2158.
9. Golden P., Dedieu H., Jacobsen K.: *Implementation and Applications of DSL Technology*. Auerbach Publications, 2008, pp. 134–137, 164–168.
10. Neus C., Boets P., Van Biesen L.: “Transfer Function Estimation of Digital Subscriber Lines”, *Proceedings of IEEE Instrumentation and Measurement Technology Conference*, Poland, 2007, pp. 1–5.
11. Starr T., Cioffi J., Silverman P.: *Understanding Digital Subscriber Line Technology*. Upper Saddle River, 1999, pp. 67–72.
12. Ysebaert G.: “Equalization and Echo Cancellation in DMT-based Systems”, Ph.D. Thesis, K.U. Leuven, 2004.
13. Golden P., Dedieu H., Jacobsen K.: *Implementation and Applications of DSL Technology*. Auerbach Publications, 2008, pp. 205–207.
14. Asymmetric Digital Subscriber Line (ADSL) transceivers. ITU, Recommendations G.992.1-G.992.5, 1999–2005, www.itu.int/rec/T-REC-G/e.
15. Very High Speed Digital Subscriber Line (VDSL) transceivers. ITU, Recommendations G.993.1-G.993.2, 2004–2006, www.itu.int/rec/T-REG-G/e.